Applied Acoustics 74 (2013) 79–88

Contents lists available at SciVerse ScienceDirect

Applied Acoustics

journal homepage: www.elsevier.com/locate/apacoust

Experimental analysis on the noise of propellers for small UAV

Giorgia Sinibaldi, Luca Marino *

Department of Mechanical and Aerospace Engineering, University of Rome "La Sapienza", Via Eudossiana 18, I-00184 Roma, Italy

ARTICLE INFO

Article history:
Received 16 December 2011
Received in revised form 7 June 2012
Accepted 20 June 2012
Available online 15 July 2012

Keywords:
Propeller noise
UAV
Tonal noise
Broadband noise

ABSTRACT

Main goal of this paper is an experimental analysis on the aeroacoustic features of propellers aimed at the propulsion of small unmanned aerial vehicles. The investigation concerns the comparison between the acoustic signature of optimized and conventional propellers driven by brushless electric motors.

This topic is particularly relevant due to the dramatic increase of the UAV market for civil and military purposes with multiple operational issues. The quietness and the efficiency of the propulsive system are key aspects in the design of advanced aerial vehicles and very often can lead to the success or failure of the mission.

In addition to the experimental research, a numerical analysis based on the compact formulation of the Ffowcs-Williams/Hawking equation and a simple model for the broadband noise, is presented and discussed.

1. Introduction

The recent increase of the number of small unmanned aerial vehicles (UAVs) has renewed the interest in the development of the propellers and puts some serious requirements on the noise produced by the propulsion system [1]. For a small propeller quietness and efficiency are appealing and some times demanding features for the success of a mini-UAV mission. Though the two characteristics are difficult to achieve simultaneously, a reduction of the noise of the propeller means sometimes the fulfillment of the UAV target and in other circumstances it is a necessary step to accomplish the regulations. On the other hand high efficiency propellers and large values of loitering times are particularly important for reconnaissance and surveillance purposes.

We will refer in particular to the paper of Gur and Rosen [2], where the principal goal was to design a quiet propeller for UAV applications. In that paper a numerical optimization was carried out to evaluate the geometric characteristics of a propeller. The results of the optimization, mainly the distributions of the chord, the pitch and the thickness were achieved under structural and aerodynamic constraints.

The main contribution of the present paper is an experimental investigation on the aeroacoustic properties of a propeller made following the guidelines reported by Gur and Rosen [2]. In particular the analysis concerns the measurement of the acoustic signature for different aerodynamic conditions. The same study is performed also on a propeller with conventional characteristics to obtain a meaningful comparison between two differently thought propulsion systems [3]. In fact the term *conventional* refers to a propeller which is not designed to reduce its noise but to achieve good aerodynamic performance, i.e. a high efficiency.

The case of zero advance ratio has been investigated on the basis of the following considerations. Micro- and mini-UAVs are usually equipped with fixed pitch propellers of small diameters powered either by alternative engines or by electric motors [2,4]. In both cases the propellers characteristics are optimized in view of the very goal at which the UAV mission is aimed. This last consideration involves that a high rpm value of the propulsion system corresponds to values of the flight speed and of the propeller diameter far from giving good efficiency results in a wide range of the advance ratio. Apart from this understandable loss of propulsive efficiency, another undesirable consequence of a working condition different from the optimal one is a high propeller noise which contrasts with the need for obtaining quiet or even silent UAVs. To the authors knowledge, little attention has been so far paid to the aeroacoustic noise of a propeller running at values of the advance ratio which correspond to poor efficiency values, in particular at fixed point, where a sizable part of the disk is stalled.

In addition to these observations, we note that, as it will be later explained in more details, the noise of a propeller is caused by different sources and is usually classified in a tonal (harmonic) and in a broadband part. A general and quite accepted definition leads to three origins for the broadband noise: noise related to the turbulence of the incoming flow (leading edge noise), noise produced by the interaction of the turbulent boundary layer over the blade surface with the trailing edge, noise generated by the possible separation of the flow on the blade airfoil [5–7]. In the peculiar case of

* Corresponding author. Tel.: + 39 06 44585735; fax: +39 06 4881759.
E-mail address: luca.marino@uniroma1.it (L. Marino).

0003-682X/$ - see front matter © 2012 Elsevier Ltd. All rights reserved.
http://dx.doi.org/10.1016/j.apacoust.2012.06.011

vanishing advance ratio the first source is almost absent [8]. On the other hand the great amount of separation of the flow could represent a significant component of the broadband noise.

The need to predict accurately the noise of propellers and rotors has made very rich the scientific and technical literature on this topic which now dates back to the 1950s. We just recall here some of the most remarkable contributions related to the present work.

From a theoretical point of view the seminal paper of Ffowcs-Williams and Hawkings [9] is fundamental and represents the base for further developments and formulations for the analysis of the aeroacoustics of rotating bodies. Among the others, we recall here some of the papers of Farassat et al. [10–12], Succi [13], Pagano et al. [14], Blandeau et al. [15] where the attention was paid to theoretical and numerical aspects. Experimental results can be found in Succi et al. [16] Dobrzinski et al. [17], Leslie et al. [18] and Roger et al. [8,19,20].

The paper is organized as follows. Next section deals with the theoretical models adopted to evaluate the aerodynamic and aeroacoustic characteristics of the propellers. Then, after the description of the experimental setup, we report and discuss the experimental results which are, in some cases, compared with the numerical data.

2. The aerodynamic and the aeroacoustic models

The aerodynamic analysis is the very first step to any experimental and theoretical investigation concerning the sound emission from propellers. In addition to the evaluation of the thrust, the torque and the efficiency which are necessary to predict the performance of the propeller, the aerodynamic calculations will provide the load distribution along the blades span which is directly responsible for part of the total noise and is a required input for the successive acoustic computations. It is thus easily understood that the accuracy of the aerodynamic analysis deeply influences the reliability of the final aeroacoustic results.

Among the many procedures available for the analysis of the propeller aerodynamics, one of the most popular and simple is based on the momentum/blade element theory [3]. Other approaches are based on the lifting line or surface theories where semi-empirical models of the wake of the propeller are usually introduced [21,22].

The simple momentum/blade-element approach is effective as shown by several authors [3,23,24] and is nowadays one of the standard methods to evaluate the thrust and the power of a propeller. We observe that in the proximity of very low values of the advance ratio, where a not negligible part of the blade is under stall conditions, the theory is corrected to take into account the maximum lift coefficient $C_{l_{max}}$ of the local section and the rotational effect of the fluid. More details can be found in the paper of Gur and Rosen [24]. Note that the simple blade element theory takes into account the experimental data of the airfoils profiles in so evaluating to some extent the viscous effects. On the other hand the methods based on the potential aerodynamics somehow suffer this limit as the advance ratio tends to very small values. In this paper we report the results of the analysis carried out by the blade-element combined with the momentum theory. A comparison between this theory and those based on a lifting line approach is shown in Marino [25].

The noise of a propeller, following a largely accepted classification, is due mainly to two different components. The first one is harmonic in the blade passing frequency *BPF*, it is almost rigorously periodic and presents a discrete frequency spectrum. The second one is a broadband contribution and has a continuos behavior in the frequency domain. The physical mechanism which gives the harmonic noise is related to the blade thickness and its surface aerodynamic loading. An additional non-linear contribution can be present and is represented as a quadrupole source. This last component is important in transonic flows and can be neglected in all the cases where the flow field around the propeller is subsonic [26].

The broadband noise is caused by the random distribution of forces over the blades surfaces and can be induced by a turbulent inflow. The oscillating pressure field can be also self induced when the evolving turbulent boundary layer interacts with the trailing edge of the blade itself.

The theoretical prediction of the harmonic noise produced by rotating blades, in particular by propellers, is classically based on the analysis of the Ffowcs-Williams/Hawkings equation [9]. As mentioned before, if the blades are thin and the pertinent Mach number falls in the subsonic regime, the quadrupole term can be neglected. The tonal contribution to the acoustic pressure is so given by the sum of a source related to blade thickness and a source linked to the aerodynamic loading and can be expressed as follows:

$$p(\mathbf{x},t) = p_t(\mathbf{x},t) + p_l(\mathbf{x},t). \tag{1}$$

In our approach we have followed the procedure of discretizing the blades in N finite elements along the span [2], as in the case of the aerodynamic blade element theory, and we have considered the overall radiation field as the contributions of N pointwise sources.

With reference to Fig. 1, a cartesian system of non dimensional coordinates $\mathbf{x} = (x, y, z)$, centered on the propeller axis and fixed in the laboratory frame, is introduced to identify the points where the observer and the sources are located. All the lengths are made non dimensional with respect to the propeller radius R.

The resulting pressure is so obtained as

$$p_t(\mathbf{x},t) = \sum_{k=1}^{N} p_{t,k}(\mathbf{x},t),$$

$$p_l(\mathbf{x},t) = \sum_{k=1}^{N} p_{l,k}(\mathbf{x},t).$$

The details of this compact formulation can be found in the papers by Farassat and Succi [10,11], here we report the formulas adopted to numerically evaluate the emitted noise

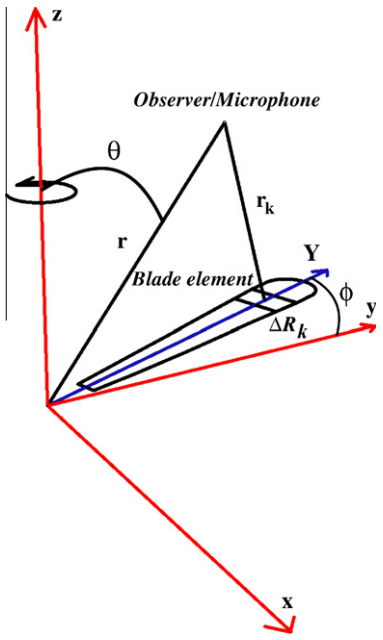

Fig. 1. Sketch of the reference frame.

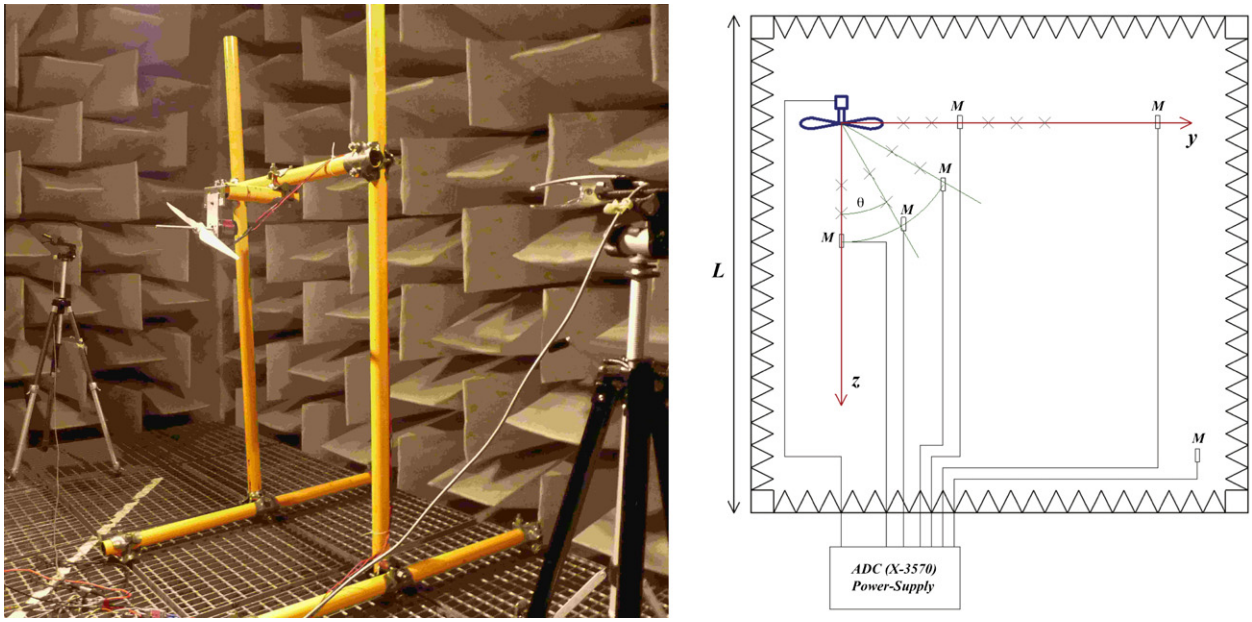

Fig. 2. Left panel: Picture of the anechoic room with an example of the experimental setup. Right panel: Sketch of the layout of the experimental setup with an array of microphone to measure the angular distribution in the near field.

$$4\pi p_{l,k}(\mathbf{x},t) = \left\{\frac{\dot{\mathbf{F}}_k\cdot\hat{\mathbf{r}}_k + \mathbf{F}_k\cdot\hat{\mathbf{r}}_k[\dot{\mathbf{M}}_k\cdot\hat{\mathbf{r}}_k/(1-M_{r_k})]}{ar_k(1-M_r)^2}\right\} + \left\{\frac{\mathbf{F}_k\cdot\hat{\mathbf{r}}_k[(1-\mathbf{M}_k\cdot\mathbf{M}_k)/(1-M_r)] - \mathbf{F}_k\cdot\mathbf{M}_k}{r_k^2(1-M_{r_k})^2}\right\}, \quad (2)$$

$$4\pi p_{t,k}(\mathbf{x},t) = \rho\frac{\partial}{\partial^2\tau^2}\left\{\frac{\Phi_k}{r_k(1-M_{r_k})}\right\}. \quad (3)$$

In Eqs. (2) and (3), ρ is the density, $\mathbf{r}_k$ is the position vector of an observer relative to the k-point noise source ($|\hat{\mathbf{r}}| = 1$), $\mathbf{F}_k$ is the aerodynamic force acting on the blade element k, of volume Φ_k. Moreover, naming a the speed of sound and $\mathbf{v}$ the velocity of the source, the Mach vector is $\mathbf{M}_k = \mathbf{v}_k/a$. The scalar quantity M_{r_k} is the component of $\mathbf{M_k}$ on $\mathbf{r_k}$. A dot over a quantity means the time derivative in the reference frame of the source of noise (retarded time).

The observer's time t and the retarded time τ are related by

$$\tau = t - r(\tau)/a.$$

We note that in Eq. (2) the first parenthesis represents the far field term while the second one is the near field contribution.

The prediction of the trailing edge broadband noise was addressed by several authors in the past and the pertinent literature is now very rich. We cite, for example, the papers [26–29] and the references therein. Among the different formulations proposed, here we report the theory based on the approach of Amiet [27,30], recently discussed and extended by Moreau et al. [8,19,20], by Pagano et al. [14] and by Blandeau et al. [15]. This approach was initially developed to predict the noise related to a turbulent flow over an airfoil [27], and then was applied also to propellers [14,20] and helicopter rotors [33]. A detailed review on the peculiar aspects of the different approaches can be found in the paper of Howe [31].

With reference to Fig. 1, for a section of the propeller blade with chord c and span ΔR the power spectral density of the trailing edge noise can be written as [15]

$$S_{pp}^{TE}(r,\theta,\omega) = \frac{B}{8\pi}\left(\frac{\omega c}{2ar}\right)^2 \Delta R\; D(\theta,\varphi)\;|I|^2\Phi_{pp}l_y. \quad (4)$$

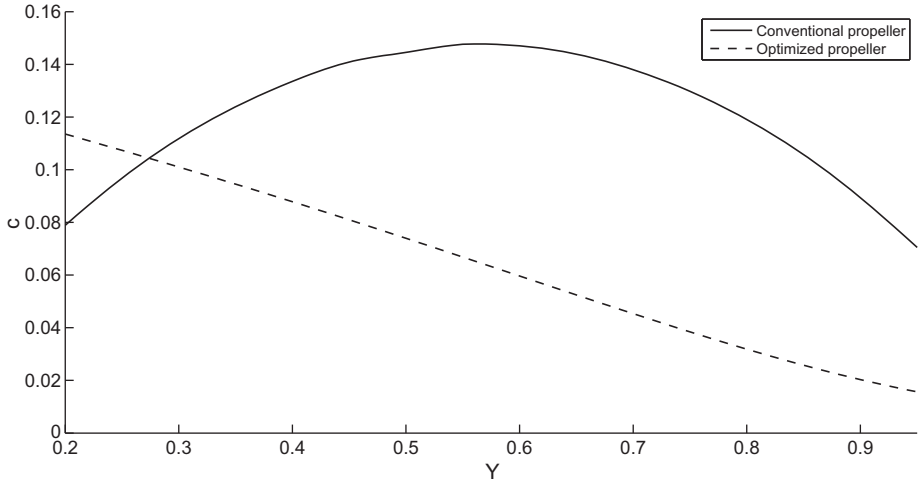

Fig. 3. Distribution of the non dimensional chord c for the conventional (continuous line) and optimized (dashed line) propeller.

In this equation B is the number of the blades, $\omega = 2\pi f$ is the angular frequency, f is the rotational frequency, $D(\theta,\varphi)$ is the directivity function, Φ_{pp} is the wall pressure power spectral density and l_y is the spanwise correlation length. The radiation integral function I has been recently discussed in Roger and Moreau [19] where it has been shown that two terms I_1,I_2 lead to its correct value. The first part I_1, as initially formulated by Amiet [27], is due to the scattering of the boundary layer at the trailing edge and corresponds to the noise of a semi-infinite flat plate. In the high frequency limit ($kc \gg 1$) this is the only significant source of trailing edge noise.

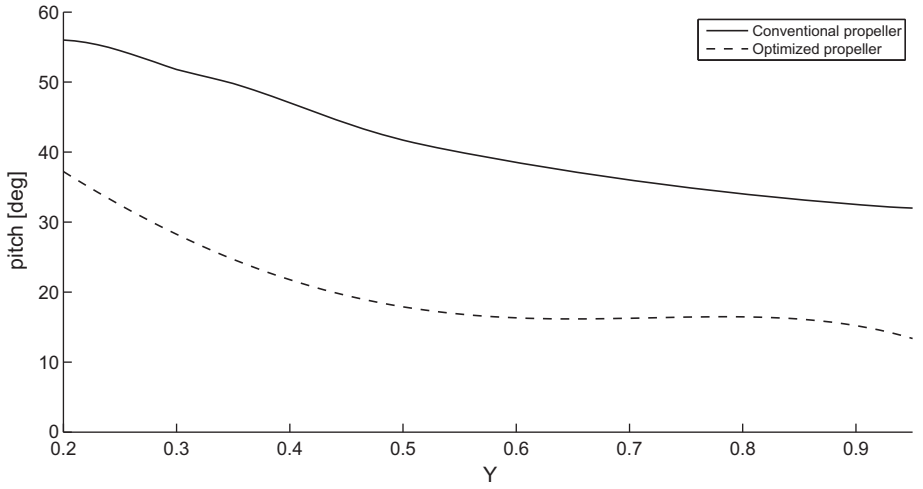

Fig. 4. Distribution of the non dimensional pitch for the conventional (continuous line) and optimized (dashed line) propeller.

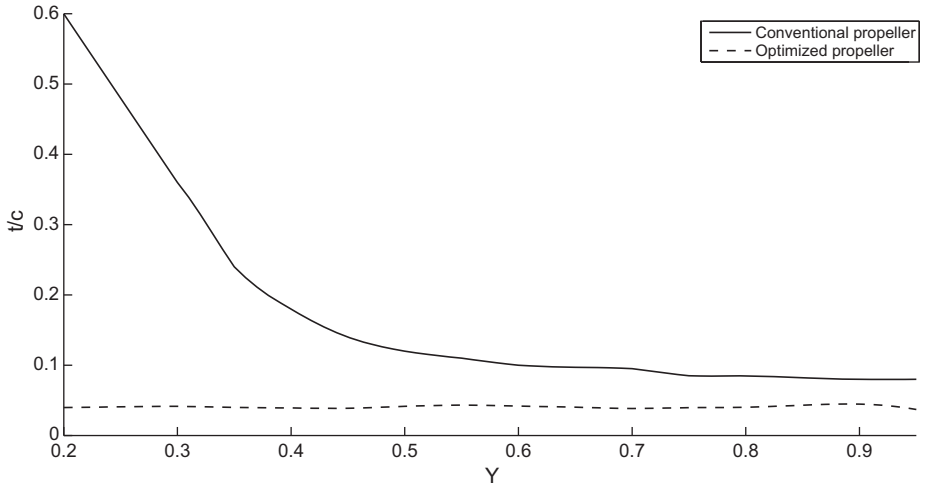

Fig. 5. Distribution of the non dimensional thickness for the conventional (continuous line) and optimized (dashed line) propeller.

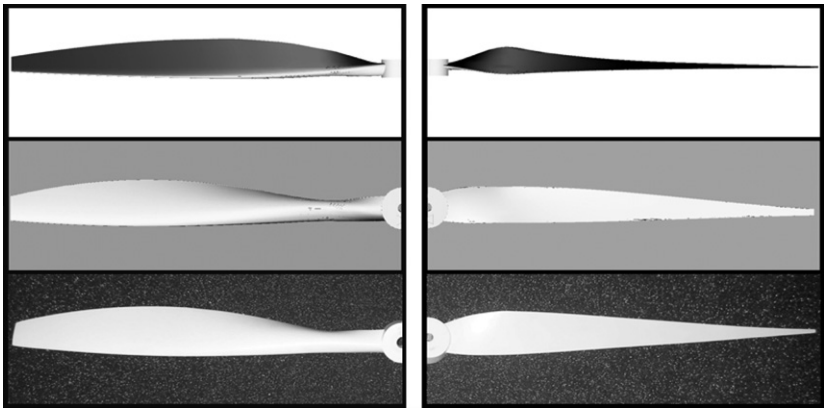

Fig. 6. Front and top views (top and middle) and pictures (bottom) of conventional (left) and optimized (right) propeller.

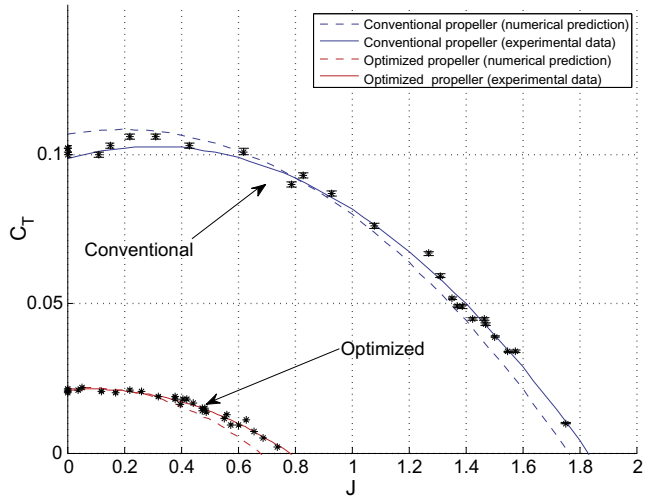

Fig. 7. Thrust coefficient C_T *versus* the advance ratio J for the conventional and the optimized propellers. Dashed lines refer to numerical predictions, continuous lines refer to a fit of the experimental data (shown with the symbols $*$ and the uncertainty bars).

When the value of the chord is of the same order of the acoustic length ($kc \leqslant 1$) also the scattering of the reflected wave on the leading edge (I_2) of the airfoil is important. Details on the importance of this correction to the Amiet theory are exposed in the paper of Roger and Moreau [19] and the complete expressions of I_1,I_2 are reported in [8,14,19].

The validity of the Amiet's model has been recently analyzed by Blandeau and Joseph [15] where the results obtained with the approximate model [27] are compared with those obtained using the exact Ffowcs-Williams and Hawkings equation. Moreover the different expressions for the directivity terms are thoroughly discussed and their equivalence has been proved.

The wall pressure power spectral density Φ_{pp} and the spanwise correlation length l_y can be obtained by experimental measurements or by numerical models. In particular the Corco's model [32] can be used for l_y, whereas different models have been proposed for Φ_{pp} ranging from the one proposed by Schklinker and Amiet [33] to the more recent one proposed by Rozenberg [34] where the effect of the adverse pressure gradient has been explicitly taken into account.

The effect of the flow separation on the broadband noise can be relevant, in particular in the study here presented where the incidence of the blades is very high for almost all the span. An experimental analysis of the noise produced by the flow over a flat plate is given by Maruta et al. [35] for high values of the angle of attack. An estimation of the power spectral density as provided by Nelson and Morfey [36] is

$$S_{pp}^{Separation}(\mathbf{x},\omega) = \left(\frac{\omega}{4\pi a r}\right)^2 \left(\rho^2 c U^3 A_s^2\right) \left(\frac{z}{r}\right)^2 \left\{\frac{C_D^2}{4}\left[\frac{2\pi U}{\omega c(1-M_r)}\right]^3 8.6\cdot 10^{-7}\right\}, \quad (5)$$

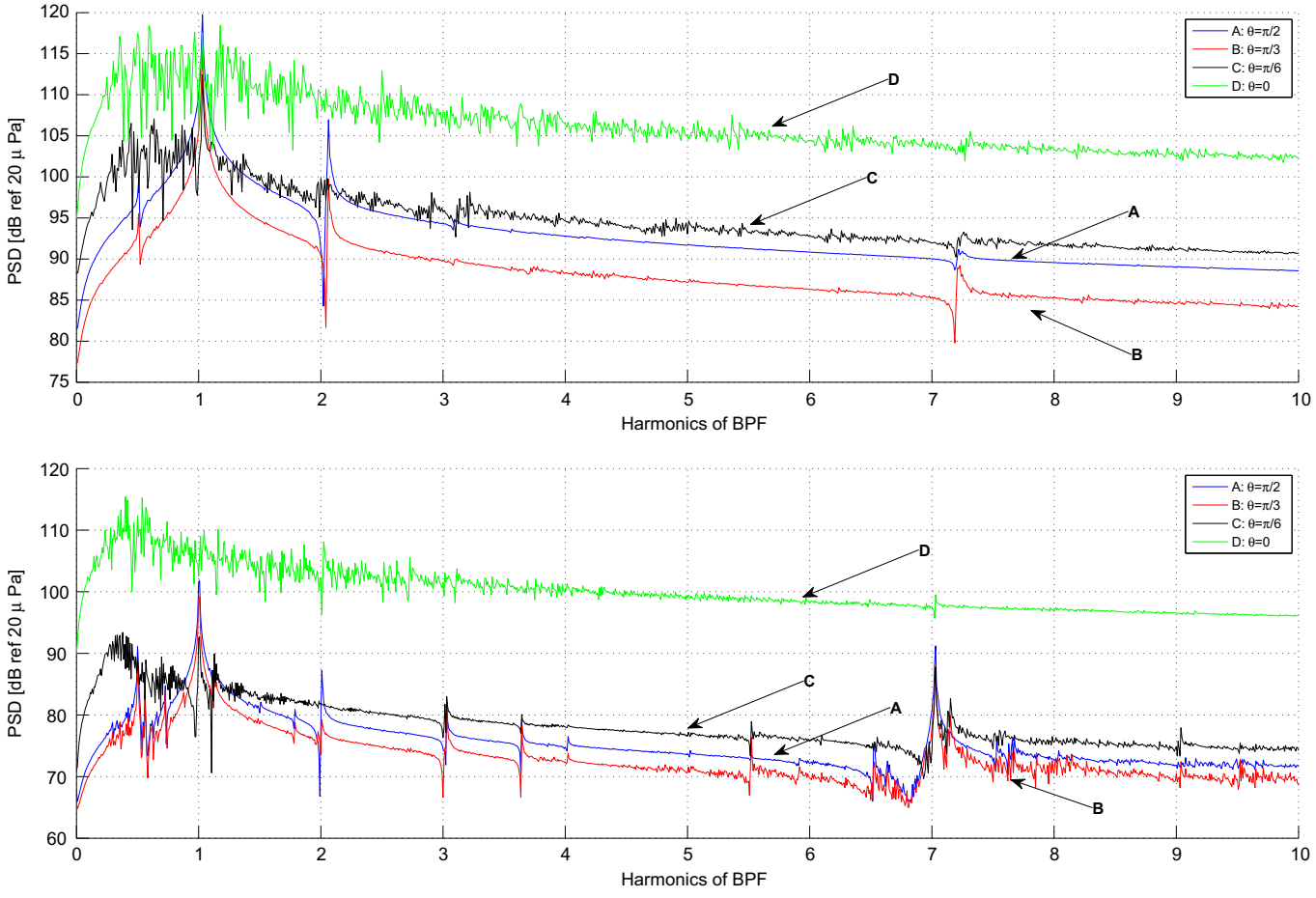

Fig. 8. Directivity effect on the power spectral density distributions (*PSD*) of the propeller/motor noise produced by the conventional (top) and optimized (bottom) propellers at $r = 2$. $T = 0.8$ N, rotational frequency $f = 16$ Hz (top), $f = 33$ Hz (bottom).

Table 1
Total sound pressure levels *OASPL* [dB] of the two systems propeller/motor at different angular positions, $r = 2$.

θ (rad)	Conventional $T = 0.8$ N	Optimized $T = 0.8$ N	Conventional $T = 1.9$ N	Optimized $T = 1.9$ N
0	93.6	96.9	108	108.7
$\pi/6$	67.6	60	84.1	85.5
$\pi/3$	54.5	46.2	71.7	82.6
$\pi/2$	57.2	42.6	74.1	72.44

where C_D is the drag coefficient, A_s the cross sectional area of the body where separation is localized and U is the incident flow speed.

The extension of the broadband theory of the airfoil to the propeller blade is achieved by means of integration of Eqs. (4) and (5) over the blade elements, as for the tonal noise analysis. The total broadband noise is then obtained by averaging over the angular position φ of the blades and by introducing a correction factor for the Doppler shift, see Pagano et al. [14] for more details.

3. Experimental setup and results

All the aeroacoustic tests have been carried out on the two-bladed propellers in the square anechoic room with size $L = 6$ m and height $h = 3$ m with a low frequency cut off of 45 Hz, located at the Research Centre of INAIL of Monteporzio Catone. In Fig. 2 a picture of the chamber and a sketch of the layout of the experimental setup are shown.

The acoustic instruments are produced by Brüel and Kjær and consist in a sound and vibration analyzer Pulse-X3570 integrated with FFT and CPB analysis tools, a Nexus 2690 amplifier and 8 free field 1/4 inch microphones type 4939 with a dynamic range 4 Hz to 25 kHz. For the measurement of the thrust of the propellers, driven by an electric brushless motor Hacker with 245 rpm/V, a three-components balance produced by Plint and Partners has been used. The rotational frequency f has been measured by means of two different and independent systems. We have adopted a frequency meter based on a light emitting diode and a receiver device which can be mounted across the propeller plane so that the ray emitted by the diode can pass through the disk of the propeller and can be intercepted by the passing blades. Furthermore we have used a telemetry system produced by the Eagle Tree Systems, which usually is employed aboard of R/C small aircraft and which provides the rotational speed of the brushless electric motor.

The aerodynamic balance has an accuracy of 0.5% of the reading, with a full scale of 50 N. The overall uncertainty on the measurement of the thrust is below 1%.

The sampling frequency of acoustic instruments spans from 0.026 Hz to 4 Hz, depending on the maximum frequency to measure and on the number of lines of discretization. In our measurements we have adopted a resolution in the range 0.026–0.25 Hz, which guarantees a quite sharp definition of the acoustic discrete tones.

As mentioned in the introduction our experimental analysis is focused on the comparison between the aeroacoustic features of

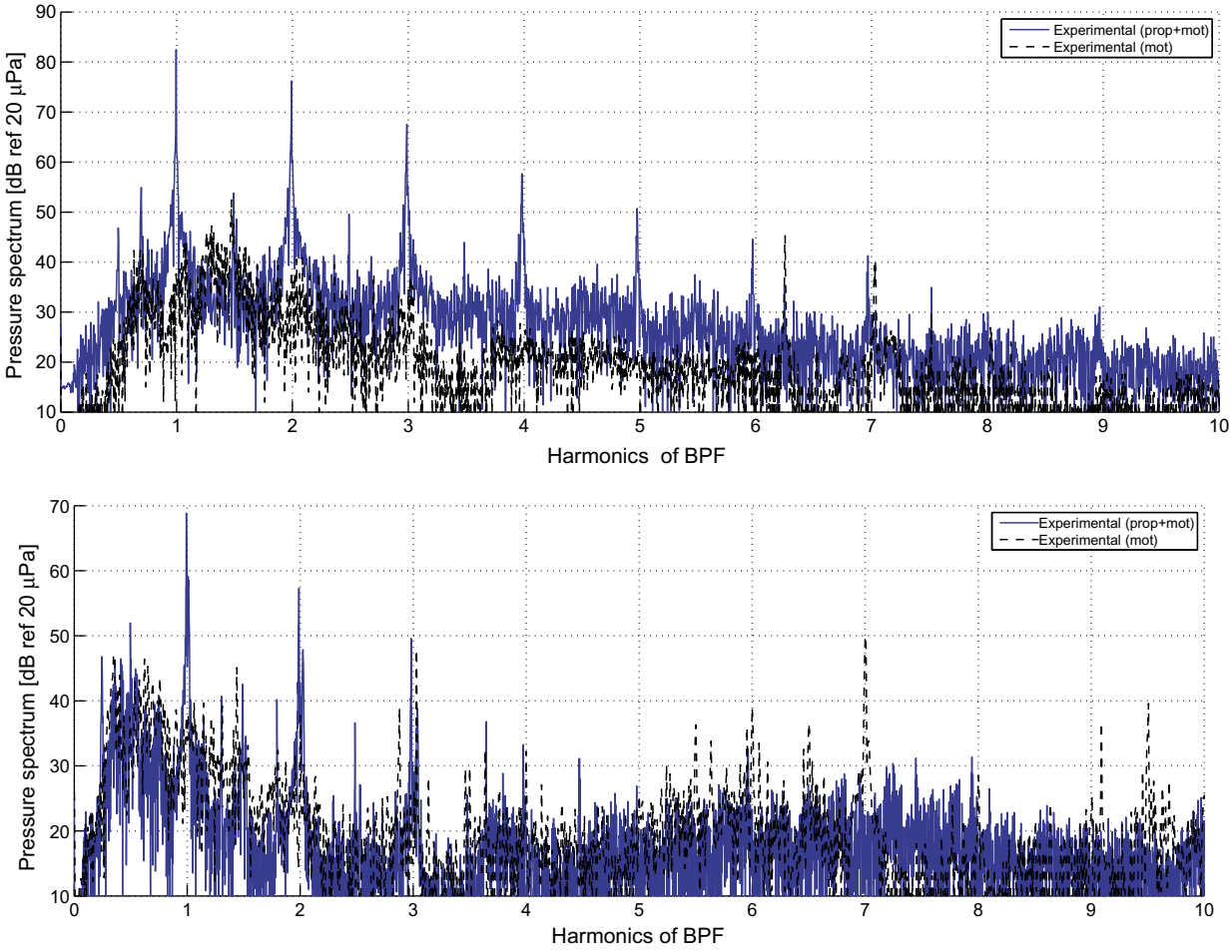

Fig. 9. Spectral distributions of the sound pressure level produced by the propeller/motor system and the motor for the conventional (top) and optimized (bottom) propellers, rotational frequency $f = 16$ [Hz] (top), $f = 33$ [Hz] (bottom). $y = 1.5$, $\theta = \pi/2$, $T = 0.8$ N.

Table 2
Comparison of total sound pressure levels *OASPL* [dB] produced by the two propellers and the electric motor. $y = 1.5$, $\theta = \pi/2$, $T = 0.8$ N.

Conventional prop./motor	80.2
Optimized prop./motor	53.4
Motor	41.9–45.3

two propellers. The propeller that we name *conventional* is not designed to achieve a reduction of the sound level and adopts an airfoil of the Clark-Y family as a basic profile. The distributions of the chord, pitch and thickness *versus* the spanwise coordinate Y of the blade (see Fig. 1) are reported in Figs. 3–5 and are obtained from Ref. [3]. The same figures report also the geometrical characteristics of the propeller *optimized* to reduce the acoustic signature, as calculated by Gur and Rosen [4]. Airfoils of the NACA-16 series have been used in this last case. The diameter D is fixed to 0.6 m for both the propellers.

Fig. 6 reports different views of the two propellers. The top and middle panels show the front and top views as obtained by the technical drawings. The bottom panels display two photos.

The first results concern the analysis of the aerodynamic performance of the two propellers. In particular the thrust coefficient $C_T = T/(\rho\ \omega^2 D^4)$, as a function of the advance ratio $J = V/(\omega\ D)$ has been experimentally evaluated in the wind tunnel of the Department of Mechanical and Aerospace Engineering of the University "La Sapienza". In the expressions of C_T and J, T is the thrust and V is the incoming flow velocity.

Fig. 7 shows the comparison between the experimental results (continuous lines and symbols $*$ with errorbars) and the numerical predictions (dashed lines) and it can be observed a satisfactory agreement for both the two propellers. If the propellers with the same diameter D have to provide the same thrust, the relation $C_{T_{conv}}\omega^2_{conv} = C_{T_{opt}}\omega^2_{opt}$, has to be accomplished and, from the analysis of the two thrust curves in Fig. 7, this means that at low values of J approximatively $\omega_{conv} \approx \omega_{opt}/2$.

The first aeroacoustic results concern the effects of the directivity on the power spectral density distribution.

We note that the signal frequency is related mainly to the perturbation of a single blade. For a two bladed propeller this frequency is twice that of the motor shaft. As a consequence in all the paper the spectral results will be plotted *versus* the harmonics of the blade passage frequency (*BPF*). Such a usual representation makes easy the comparison between propellers rotating with different angular speeds. For the sake of clarity, only the first harmonics of *BPF* are shown, where the tonal contribution of the noise is more evident.

Fig. 8 shows the power spectral density obtained for four different angular positions θ of the microphones with respect to the axis z of the propeller, keeping constant the distance $r = 2$ from the axes origin (see Fig. 1). For both the two propellers the data measured in the rotational plane show the marked contribution of the tonal component of the noise. As the observer/microphone moves toward the axial location (decreasing θ) the harmonic contribution becomes less evident, while the broadband term increases and overcomes the discrete tones. For $\theta \leqslant \pi/6$ the blade tonal component is almost hidden by the prevailing broadband source.

This results agree with the theoretical prediction based on the models reported in the previous sections. In particular it has been shown in Refs. [8,14,15,19] that the broadband trailing edge noise exhibits a more or less marked minimum in correspondence of the rotational plane ($\theta = \pi/2$).

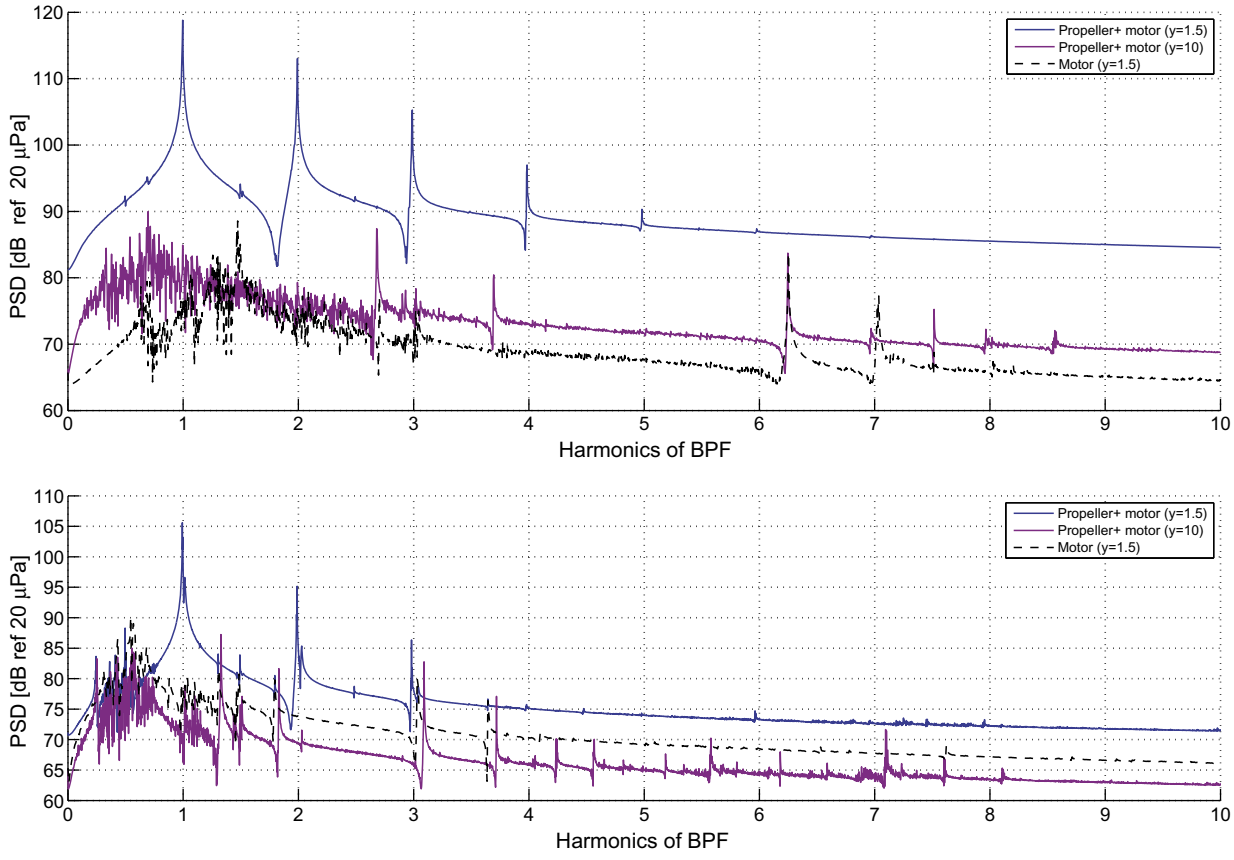

Fig. 10. Power spectral density distributions (*PSD*) of the prop/motor and motor noise produced by the conventional (top) and optimized (bottom) propellers, rotational frequency $f = 16$ Hz (top), $f = 33$ Hz (bottom). $T = 0.8$ *N*, $\theta = \pi/2$.

We recover this behavior also for the overall sound pressure level (*OASPL*) and also at different values of the thrust of the propellers. Table 1 summarizes the directivity of the total sound pressure levels at $r = 2$. When the microphone moves from the rotational plane angular position ($\theta = \pi/2$) toward the axial location ($\theta = 0$) we recognize initially a very limited change in the sound pressure levels for both the two propellers. The conventional one shows a small reduction, while the optimized propeller exhibits a small increase. For $\theta < \pi/3$ both the propellers display a marked increase of the total noise.

A further note regards the difference of the *OASPL* between the two propellers. At $\theta = \pi/2$ the optimized propeller is actually quieter than the conventional one, but this difference falls to almost zero when the microphone is in the wake of the propeller ($\theta = 0$).

It is clear that a better comparison between the tonal contribution of the two propellers is achieved when the measurements are carried out in proximity of the rotational plane. Moreover the characteristics of the low noise propeller was obtained by Gur et al. [4] by minimizing only the harmonic term of the noise.

Following these considerations in the sequel we limit our analysis taking into account only the data obtained in the rotational plane of the propellers ($z = 0, \theta = \pi/2$) at different locations on the y axis.

Fig. 9 shows a comparison between the experimental sound pressure spectra produced by the propeller/motor system and by the motor without the propeller. The comparison is given for both the conventional and the optimized configurations at $y = 1.5$, at the same value of the thrust produced.

It can be observed that when the propeller is removed, the acoustic behavior of the motor changes, even if the rotational frequency f is kept fixed, due to a minor loading on the shaft of the motor. So, in principle, the two sets of measurements should not be comparable but, in any case, it is interesting to carry on the analysis to have an insight of the contribution of the motor to the total noise and to obtain a first rough correction of the experimental data. A marked difference between the complete propulsion apparatus and the motor can be noticed at the first multiples of the blade passing frequency where the tonal noise of the propeller is dominant. For the remaining frequency the acoustic signature of the system propeller/motor is caused by the noise of the motor and the broadband noise of the propeller. Discrete tones can be observed also at frequencies which are not multiples of the fundamental harmonic of the *BPF*. This phenomenon is more evident for the optimized propeller than for the conventional one and can be related to a small tonal component of the noise of the motor. The comparison between the two spectra exhibits, as expected, a lower level of noise produced by the optimized propeller with respect to the conventional one. Moreover the difference between the noise of the motor and that of the propeller/motor decreases in the optimized case as an additional evidence of a lower contribution of the propeller.

A quantitative comparison of the sound pressure levels which takes into account all the frequency domain (0–25 kHz) is reported in Table 2. The total sound pressure level of the optimized propeller is more than 10 dB lower with respect to the other one. The *OASPL* of the motor assumes two lightly different values due to the two angular velocities corresponding to 16 Hz and 33 Hz for the conventional and optimized propeller, respectively.

We observe that the first blade passage frequency of the conventional propeller, when the thrust is $T = 0.8$ N, is $f_B = 32$ Hz which

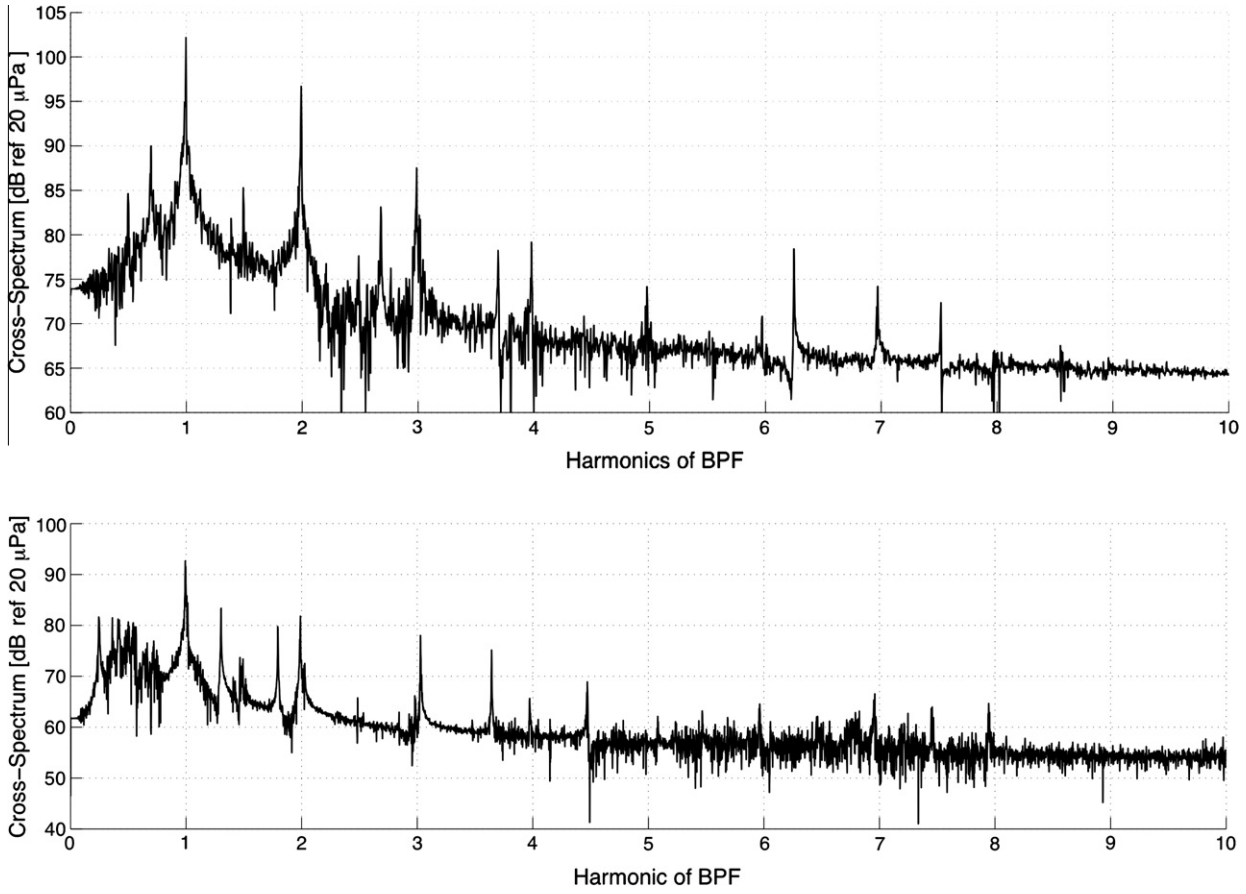

Fig. 11. Cross-spectrum of the near and far fields noise for the conventional (top) and optimized (bottom) propellers, rotational frequency $f = 16$ Hz (top), $f = 33$ Hz (bottom). $y = 1.5$, $\theta = \pi/2$, $T = 0.8$ N.

is a little bit below the cutoff frequency F_{cutoff} = 45 Hz of the anechoic room.

In this situation the complete acoustic energy absorption by the walls of the room is not guaranteed and the reflection of the acoustic waves could induce disturbance on the measurements. In fact above the cutoff frequency the anechoic wedges have a coefficient of energy absorption at normal incidence greater than 0.99. We assume that the error is negligible due to the very close value of this frequency with respect to the cutoff frequency and to the usual smooth decrease of the absorption coefficient for the acoustically insulating materials generally adopted in the anechoic rooms [38].

Fig. 10 shows the power spectral density of the two propellers as measured at two different positions. The values at y = 1.5 correspond to the near field noise while at y = 10 the measurement gives the far field [37]. The acoustic power content in the near field is localized at the first tonal frequencies where the deterministic noise produced by the passing blades overcomes the other contributions. It is worth noting that the near field *PSD* of the motor is of the same order of the overall contribution evaluated in the far field. This is a further proof of the predominant effect of the propeller noise. Furthermore a series of discrete peaks which are directly related to the motor can be observed in the power spectral distributions. These tones are quite clearly recognizable in the measurements of the motor and in the far field of the propeller/motor while are less evident in the near field where the noise produced by the propeller blades is dominant.

In Fig. 11 the cross-spectra of the near-far signals are shown. Due to its intrinsic meaning the Fourier transform of the cross-correlation of the two time signals gives the correlation of the two fields in the frequency domain. A correlation of the tonal noise is clearly observed at the first few harmonics, while at higher frequencies the correlation is related to different sources as in the case of the above mentioned tones of the motor.

The last results concern the comparison of the experimental data against the numerical prediction based on the simple mathematical models presented in Section 2. Fig. 12 displays the sound pressure level spectra at y = 1.5 when the thrust produced is equal to T = 1.9 N. In presenting the experimental data we have considered the effect of the noise of the motor in terms of its mean acoustic pressure. In particular we have discretized the frequency domain in bandwidths equal to the blade passing frequency and centered on the first harmonic of the *BPF* and its multiples. The average values in these bandwidths have been subtracted to the total experimental noise. The resulting signal is shown in Fig. 12 together with the motor and the numerical predictions. It can be observed that the corrections due to the motor noise are in any case very small and the differences between the sound pressure level of the propeller/motor and the corrected propeller are almost negligible.

For the numerical data we present either the noise corresponding only to the tonal contribution and the total noise which takes into account also the broadband term. The agreement is quite satisfactory, in particular near to the blade passing frequencies where the analysis restricted to the tonal component already predicts quite well the values of the peaks of the sound level. The extension of the numerical model to the broadband contribution increases the agreement to almost all the frequency domain reported. The differences between the experimental and numerical distributions can be recognized partially in the electric motor whose noise has not been completely and effectively evaluated in the post processing procedure. Moreover additional sources of uncertainties are given in the broadband noise model. In particular the proper

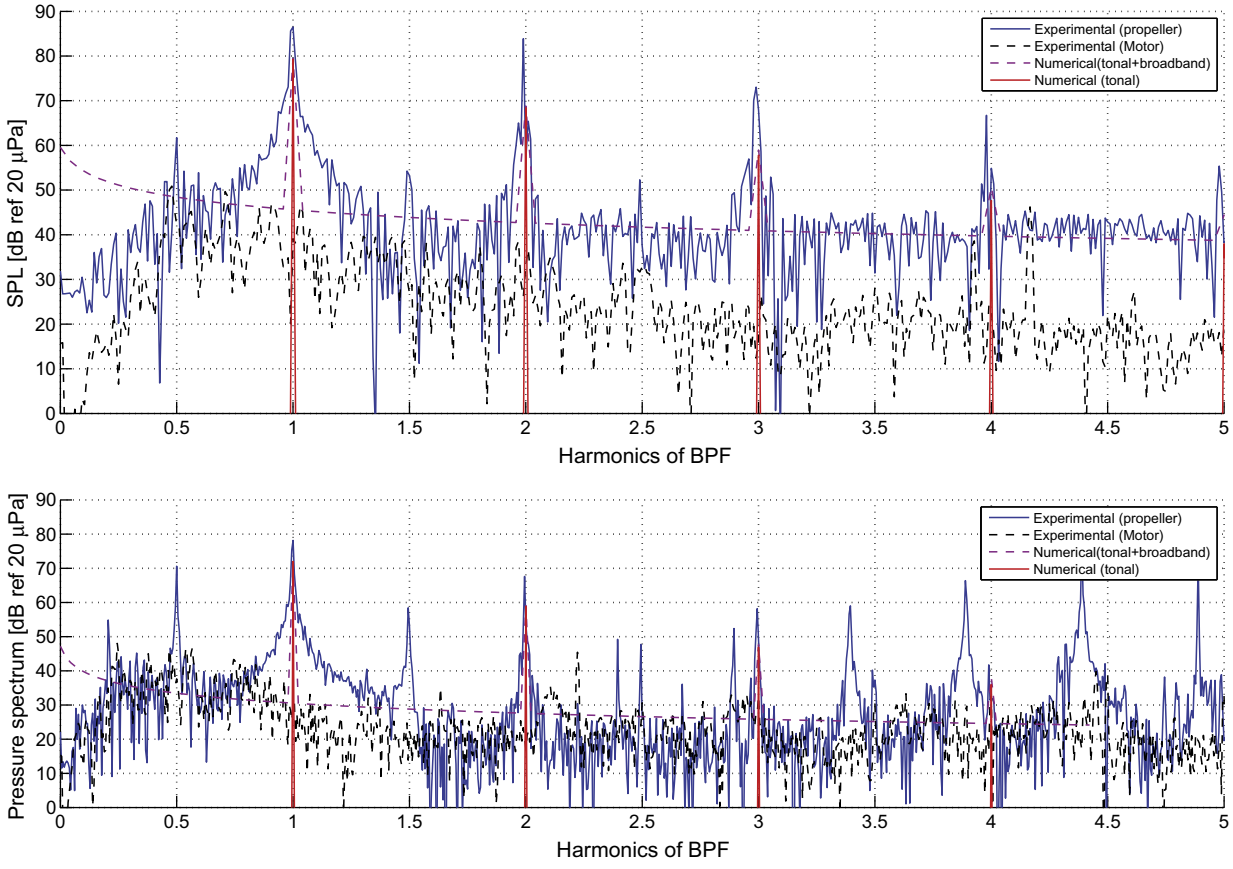

Fig. 12. Comparisons between the experimental and the numerical spectral distributions of the pressure sound level produced by the conventional (top) and the optimized (bottom) propeller. Rotational frequency f = 24 Hz (top), f = 45 Hz (bottom). T = 1.9 N, y = 1.5, $\theta = \pi/2$.

Table 3
OASPL [dB] for the two propellers at $\theta = \pi/2$.

	Experiments		Numerical prediction	
	Conventional	Optimized	Conventional	Optimized
T = 0.8 N				
y = 1.5	80.2	53.36	70.4	61.5
y = 10	31	28.8	36	27
T = 1.9 N				
y = 1.5	95.53	83.5	83.4	78.5
y = 10	42.9	37.9	39	38.1

pressure gradient over the blades should be experimentally evaluated to achieve a reliable power spectrum density of the wall pressure. We do not go into more details on this last numerical aspect that actually was thoroughly studied by Roger and Moreau [19].

Table 3 shows the total sound pressure level *OASPL* at different positions and at two different values of the thrust. In addition to the experimental values we provide the results based on the numerical prediction and a satisfactory agreement can be oberved. It is worth to note that at the lower value of thrust the noise of the optimized propeller is significantly lower than that of the conventional one, coherently with the theoretical prediction reported by Gur and Rosen [2]. When the thrust is increased to $T = 1.9$ N the noise of the two propellers becomes of the same order of magnitude. Furthermore in the far field the differences between the propellers are very small. In the authors opinion the main reason of this behavior is the relevant increase of the vibrations observed for the optimized propeller, which has blades with a smaller mean thickness and so a higher flexibility than the conventional ones. Moreover the effect of the broadband noise plays an important role, particularly in the far field. This effect has not been considered in the numerical analysis which shows a lower agreement as a consequence.

4. Conclusions

We have presented and discussed the results of an experimental analysis of the aeroacoustic characteristics of two different propellers. The main target was to establish the effectiveness of a design aimed at a low acoustic signature with respect to a propeller developed with the purpose of good aerodynamic and structural properties. In particular the aerodynamic and geometrical features of the acoustically optimized propeller has been obtain by a previous theoretical analysis [2]. The comparison between the two propellers has given interesting results and puts in evidence the better acoustic behavior of the optimized propeller with respect to a conventional one at least for the deterministic tonal contribution. In the former case some limits have been observed when the rotational frequency is increased to obtain higher thrust values. The limited mean thickness of the blade of this propeller results in a significant vibrations phenomena which cause an increase in the production of noise that becomes comparable to that of the conventional design. This effect has not been taken into account in the numerical models here adopted to evaluate the aeroacoustic characteristics.

Future activities foresee an on board analysis of the performance of these propellers. In particular the acoustic signature has to be evaluated when the propulsion system will be integrated on a medium size UAV so that also the frame noise will be taken into account and evaluated in comparison to the noise of the propulsion apparatus.

Acknowledgement

The authors thank Dr. R. Sisto of INAIL for the availability of the anechoic room and her fruitful suggestions.

References

[1] Holmes JB, Durham MH, Tarry SE. Small aircraft transportation system concept and technologies. J Aircraft 2004;41:26–35.
[2] Gur O, Rosen A. Design of a quiet propeller for an electric mini unmanned air vehicle. J Prop Power 2009;25:717–28.
[3] McCormick BW. Aerodynamics, aeronautics, and flight mechanics. John Wiley & Sons; 1995.
[4] Gur O, Rosen A. Optimizing electric propulsion systems for unmanned aerial vehicles. J Aircraft 2009;46:1340–53.
[5] Glegg SAL, Baxter SM, Glendinning AG. The prediction of broadband noise from wind turbines. J Sound Vib 1987;118(2):217–39.
[6] Magliozzi B, Hanson DB, Amiet RK. Propeller and propfan noise. Aeroacoust Flight Veh: Theory Practice 1991;1:1–64.
[7] Brooks TF, Schlinker RH. Progress in rotor broadband noise research. Vertica 1983;7:287–307.
[8] Roger M, Moreau S. Broadband self-noise from loaded fan blades. AIAA J 2004;42:536–44.
[9] Ffowcs-Williams JE, Hawkings DL. Sound generation by turbulence and surfaces in arbitrary motion. Philos Trans Roy Soc 1969;264:321.
[10] Farassat F, Succi GP. A review of propeller discrete frequency noise prediction technology with emphasis on two current methods for time domain calculations. J Sound Vib 1980;71:399–419.
[11] Farassat F. Linear acoustic formulas for calculation of rotating blade noise. AIAA J 1981;19:1122–30.
[12] Farassat F, Brentner KS. The acoustic analogy and the prediction of the noise of rotating blades. Theoret Comput Fluid Dyn 1998;10:155–70.
[13] Succi GP. Design of quiet efficient propellers. In: SAE business aircraft meeting; 1979.
[14] Pagano A, Barbarino M, Casalino D, Federico L. Tonal and broadband noise calculations for aeroacoustic optimization of a pusher propeller. J Aircraft 2010;47(3):835–48.
[15] Blandeau VP, Joseph PF. Validity of Amiet's model for propeller trailing-edge noise. AIAA J 2011;49(5):1057–66.
[16] Succi GP, Munro DH, Zimmer JA. Experimental verification of propeller noise prediction. AIAA J 1980;20(11):1483–91.
[17] Dobrzynski WM, Heller HH, Powers JO, Densmore JE. DFVLR/FAA propeller noise tests in the German–Dutch wind tunnel DNW'. FAA rep; 1986 [AEE 86-3].
[18] Leslie A, Wong KC, Auld D. Broadband noise reduction on a mini-UAV propeller. In: 14th AIAA/CEAS aeroacoustic conference; 2008.
[19] Roger M, Moreau S. Back-scattering correction and further extensions of Amiet's trailing-edge noise model. Part 1: Theory. J Sound Vib 2005;4286(3):477–506.
[20] Moreau S, Roger M. Competing broadband noise mechanisms in low-speed axial fans. AIAA J 2007;45(1):48–57.
[21] Favier D, Maresca C, Ettaouil A. Numerical and experimental investigation of isolated propeller wakes in axial flight. J Aircraft 1989;26:837–46.
[22] Marretta RA, Daví G, Milazzo A, Lombardi G, Carley M. A procedure for the evaluation of installed propeller noise. J Sound Vib 2001;244(4):697–716.
[23] Gur O, Rosen A. Propeller performance at low advance ratio. J Aircraft 2005;42(2):435–41.
[24] Gur O, Rosen A. Comparison between blade-element models of propellers. Aeron J 2008;112:689–704.
[25] Marino L. Experimental analysis of UAV-propeller noise. In: 16th AIAA/CEAS aeroacoustic conference; 2010.
[26] Ffowcs Williams JE, Hall LH. Aerodynamic sound generation by turbulent flow in the vicinity of a scattering half-plane. J Fluid Mech 1970;40(4):657–70.
[27] Amiet RK. Acoustic radiation from an airfoil in a turbulent stream. J Sound Vib 1975;41(4):407–20.
[28] Brooks TF, Hodgson TH. Trailing edge noise prediction from measured surface pressures. J Sound Vib 1981;78(1):69–117.
[29] Brooks TF, Marcolini MA. Scaling of airfoil self-noise using measured flow parameters. AIAA J 1985;23:207–13.
[30] Amiet RK. Noise due to turbulent flow past a trailing edge. J Sound Vib 1976;47(3):387–93.
[31] Howe MS. A review of the theory of trailing edge noise. J Sound Vib 1978;61(3):437–65.
[32] Corcos GM. The structure of turbulent pressure field in boundary-layer flows. J Fluid Mech 1964;18(3):353–78.
[33] Schlinker RH, Amiet RK. Helicopter rotor trailing edge noise. NASA CR-3470; 1981.
[34] Rozenberg Y, Roger M, Moreau S. Fan blade trailing-edge noise prediction using RANS simulations. J Acoust Soc Am 2008;123(5):3688.
[35] Maruta Y, Kotake S. Separated flow noise of a flat plate. Report No. 592, vol. 46. Tokyo: University, Institute of Space and Aeronautical Science; 1981. p. 105–74.
[36] Nelson PA, Morfey CL. Aerodynamic sound production in low speed flow ducts. J Sound Vib 1981;79(2):263–89.
[37] Leggat LJ, Siddon TE. Experimental study of aeroacoustic mechanism of rotor–vortex interactions. J Sound Vib 1978;64:1070–7.
[38] Everest FA. Master handbook of aeroacoustics. McGraw-Hill; 2001.